



NASA-CR-201445

**AIAA 95-2339**

## **A Global Interpolation Function (GIF) Boundary Element Code for Viscous Flows**

O. Lafe  
OLTech Corporation  
Innovative Computing Group  
Chesterland, OH

D.R. Reddy  
NASA-Lewis Research Center  
Cleveland, OH

A. H-D. Cheng  
University of Delaware  
Newark, DE

**31st AIAA/ASME/SAE/ASEE  
Joint Propulsion Conference and Exhibit  
July 10-12, 1995/San Diego, CA**

For permission to copy or republish, contact the American Institute of Aeronautics and Astronautics  
370 L'Enfant Promenade, S.W., Washington, D.C. 20024

# A GLOBAL INTERPOLATION FUNCTION (GIF) BOUNDARY ELEMENT CODE FOR VISCOUS FLOWS

O. Lafe

OLTech Corporation  
Innovative Computing Group  
11795 Sherwood Trail  
Chesterland, Ohio 44026

D.R. Reddy

NASA-Lewis Research Center  
Cleveland, Ohio 44135

A. H-D. Cheng

Department of Civil Engineering  
University of Delaware  
Newark, Delaware 19716

## Abstract

Using global interpolation functions (GIFs), boundary element solutions are obtained for two- and three-dimensional viscous flows. The solution is obtained in the form of a boundary integral plus a series of global basis functions. The unknown coefficients of the GIFs are determined to ensure the satisfaction of the governing equations at selected collocation points. The values of the coefficients involved in the boundary integral equations are determined by enforcing the boundary conditions. Both primitive-variable and vorticity-velocity formulations are examined.

## Introduction

The boundary element method (BEM) has traditionally been applied to problems governed by linear differential equations. At the core of the basic BEM computational process is the fundamental solution (also referred to as the free-space Green's function) defined as the impulse response of the governing equation to a unit action. This fundamental solution is either too difficult or impossible to derive for practical nonlinear problems. Recently, with the introduction of the so-called *Dual Reciprocity* techniques (see e.g., Nardini & Brebbia [1982]; Brebbia et al., [1991]; Partridge et al., [1992]; Cheng et al.,

[1993]; Lafe [1993]; Lafe & Cheng [1994]), the method is being proposed for certain classes of nonlinear problems.

Using the *Dual Reciprocity* approach, a given problem is typically decomposed into two parts - the linear and nonlinear portions. The solution to the linear portion is represented by a boundary integral whose kernel consists of the fundamental solution to the linear governing equation. The nonlinear part is represented by either 1) local basis functions (Brebbia et al., [1991]); or 2) global interpolation functions (GIFs) (Lafe [1993]). In either case, the boundary integral expressions and interpolation functions contain coefficients whose values are to be determined by enforcing the boundary conditions. When the "direct BEM" approach is followed the unknown coefficients are in essence the unknown physical variables (velocity components, pressure, temperature) of the problem. On the other hand, using the "indirect BEM" approach, the unknowns are the weights/strengths of the boundary sources/dipoles and the local/global interpolating functions. The computational intensity of the indirect approach is much less than for the direct.

In this paper, we report the formulation and development of GIF-based indirect BEM codes for two- and three-dimensional incompressible viscous flows.

## Governing Equations

### 2D Primitive Variable Formulation

The governing equations are

$$\frac{\partial u_x}{\partial x_x} + \frac{\partial v_x}{\partial y_x} = 0 \quad (1)$$

$$u_x \frac{\partial u_x}{\partial x_x} + v_x \frac{\partial u_x}{\partial y_x} = -\frac{1}{\rho} \frac{\partial p_x}{\partial x_x} + \frac{\mu}{\rho} \left( \frac{\partial^2 u_x}{\partial x_x^2} + \frac{\partial^2 u_x}{\partial y_x^2} \right) \quad (2)$$

$$u_x \frac{\partial v_x}{\partial x_x} + v_x \frac{\partial v_x}{\partial y_x} = -\frac{1}{\rho} \frac{\partial p_x}{\partial y_x} + \frac{\mu}{\rho} \left( \frac{\partial^2 v_x}{\partial x_x^2} + \frac{\partial^2 v_x}{\partial y_x^2} \right) \quad (3)$$

where  $(u_x, v_x)$  are the velocity components, and  $p_x$  is the pressure. Let  $x = x_x/L$ ;  $y = y_x/L$ ;

$u = u_-/\bar{v}_-; v = v_-/\bar{v}_-; p = p_-/(\rho\bar{v}_-^2)$ . With these the governing equations become:

$$\frac{\partial u}{\partial x} + \frac{\partial v}{\partial y} = 0 \quad (4)$$

$$u \frac{\partial u}{\partial x} + v \frac{\partial u}{\partial y} = -\frac{\partial p}{\partial x} + \frac{1}{R_e} \left( \frac{\partial^2 u}{\partial x^2} + \frac{\partial^2 u}{\partial y^2} \right) \quad (5)$$

$$u \frac{\partial v}{\partial x} + v \frac{\partial v}{\partial y} = -\frac{\partial p}{\partial y} + \frac{1}{R_e} \left( \frac{\partial^2 v}{\partial x^2} + \frac{\partial^2 v}{\partial y^2} \right) \quad (6)$$

where  $R_e = \rho\bar{v}_-L/\mu$ .

By taking the divergence of the momentum equation and using the continuity equation, we obtain a PDE for the pressure in the form:

$$\nabla^2 p = 2 \left( \frac{\partial u}{\partial x} \frac{\partial v}{\partial y} - \frac{\partial u}{\partial y} \frac{\partial v}{\partial x} \right) \quad (7)$$

**BEM-GIF Formulation** The solution for a flow variable  $\zeta$  is decomposed into two parts ( $\zeta_0$  and  $\zeta_1$ ), such that

$$\zeta = \zeta_0 + \zeta_1$$

and  $\zeta_0$  is the solution to the convection-free problem

$$\nabla^2 \zeta_0 = 0$$

Therefore, the correction  $\zeta_1$  is the addition required such that the full governing equation is satisfied. The part  $\zeta_0$  can be modeled to a high degree of precision by boundary integral equations. The correction  $\zeta_1$  is represented by a series formed by global basis functions.

The fundamental solution for convection-free two-dimensional must satisfy

$$\nabla^2 g(\mathbf{x}, \mathbf{x}') = 2\pi\delta(\mathbf{x}, \mathbf{x}')$$

where  $\delta$  is the Dirac delta function applied at point  $\mathbf{x} = (x, y)$ , and felt at the point  $\mathbf{x}' = (x', y')$ . The closed form solution for  $g$  is easily shown to be (Jaswon & Symm [1977])

$$g = \ln r$$

where  $r = |\mathbf{x} - \mathbf{x}'|$ .

We distribute sources (plus vortices for the velocities) of unknown strength  $\omega$  on the flow boundary  $\Gamma$ . The combination of sources and vortices for the velocity components is important because of the need to automatically conserve mass. The solution for  $u, v, p$  is written as:

$$u(\mathbf{x}) = \int_{\Gamma} \{ \omega_1(\mathbf{x}') g_{11}(\mathbf{x}, \mathbf{x}') + \omega_2(\mathbf{x}') g_{12}(\mathbf{x}, \mathbf{x}') \} d\Gamma + \sum_k \{ \beta_{1k} \Phi_{k11}(\mathbf{x}) + \beta_{2k} \Phi_{k12}(\mathbf{x}) \} \quad (8)$$

$$v(\mathbf{x}) = \int_{\Gamma} \{ \omega_1(\mathbf{x}') g_{21}(\mathbf{x}, \mathbf{x}') + \omega_2(\mathbf{x}') g_{22}(\mathbf{x}, \mathbf{x}') \} d\Gamma + \sum_k \{ \beta_{1k} \Phi_{k21}(\mathbf{x}) + \beta_{2k} \Phi_{k22}(\mathbf{x}) \} \quad (9)$$

$$p(\mathbf{x}) = \int_{\Gamma} \omega_3(\mathbf{x}') g_{33}(\mathbf{x}, \mathbf{x}') d\Gamma + \sum_k \beta_{3k} \Phi_{k33} \quad (10)$$

in which  $\mathbf{x} = (x, y)$ ,  $g_{ij}$  are associated with the fundamental solutions of the convection-free problem, and  $\Phi_{kij}$  are global interpolation bases. For mass to be automatically conserved the free-space functions and GIFs must satisfy the following conditions:

$$\frac{\partial g_{12}}{\partial x} = -\frac{\partial g_{22}}{\partial y} \quad (11)$$

$$\frac{\partial g_{21}}{\partial y} = -\frac{\partial g_{11}}{\partial x} \quad (12)$$

$$\frac{\partial \Phi_{k12}}{\partial x} = -\frac{\partial \Phi_{k22}}{\partial y} \quad (13)$$

$$\frac{\partial \Phi_{k21}}{\partial y} = -\frac{\partial \Phi_{k11}}{\partial x} \quad (14)$$

For example, with  $g_{11} = g_{22} = g = \ln r$ , we have

$$g_{12} = \frac{\pi}{2} - \arctan \left\{ \frac{y - y'}{x - x'} \right\}$$

$$g_{21} = \arctan \left\{ \frac{y - y'}{x - x'} \right\}$$

Note that when  $g_{ii}$  is a source, the associated functions required to ensure mass conservation  $g_{ij}$  ( $i \neq j$ ) turn out to be vortices.

Similarly, using hyperbolic cosine global bases, with  $\Phi_{k11} = \Phi_{k22} = \cosh(m_k x) \cosh(n_k y)$  ( $m_k, n_k = 1, 2, 3, \dots$ ) we have

$$\Phi_{k12} = -\frac{n_k}{m_k} \sinh(m_k x) \sinh(n_k y)$$

$$\Phi_{k21} = -\frac{m_k}{n_k} \sinh(m_k x) \sinh(n_k y)$$

The solutions for other auxiliary bases  $\Phi_{kij}$  ( $i \neq j$ ) for given  $\Phi_{kii}$  are shown below:

• **Polynomial GIF**

$$\begin{aligned}\Phi_{k11} = \Phi_{k22} &= x^m y^n \\ \Phi_{k12} &= -\frac{m}{n+1} x^{m-1} y^{n+1} \\ \Phi_{k21} &= -\frac{n}{m+1} x^{m+1} y^{n-1}\end{aligned}$$

• **Trigonometric GIF**

$$\begin{aligned}\Phi_{k11} = \Phi_{k22} &= \cos(mx) \cos(ny) \\ \Phi_{k12} &= \frac{n}{m} \sin(mx) \sin(ny) \\ \Phi_{k21} &= \frac{m}{n} \sin(mx) \sin(ny)\end{aligned}$$

• **Radial GIF**

$$\begin{aligned}\Phi_{k11} = \Phi_{k22} &= \frac{r^m}{m} \quad m = 2(n+1) \\ \Phi_{k12} &= -r^m \left\{ (x - x_n)(y - y_n) + \frac{r}{2} \right\} \\ \Phi_{k21} &= -r^m \left\{ (x - x_n)(y - y_n) + \frac{r}{2} \right\}\end{aligned}$$

If  $n_d$  terms are selected in the GIF series, then the coefficients  $\beta_{ik}$  ( $i = 1, 2, 3; k = 1, 2, \dots, n_d$ ) are determined by enforcing the momentum equations at  $n_d$  collocation points. The strengths  $\omega_i$  ( $i = 1, 2, 3$ ) of the sources/vortices are determined by enforcing the boundary conditions at selected  $n_b$  boundary nodes. The details of the numerical implementation is outlined later.

## 2D Streamfunction-Vorticity Formulation

In two-dimensional flow, the streamfunction  $\Psi$  and vorticity  $\zeta$  are defined by

$$\begin{aligned}u &= \frac{\partial \Psi}{\partial y} \\ v &= -\frac{\partial \Psi}{\partial x} \\ \zeta &= \frac{\partial u}{\partial y} - \frac{\partial v}{\partial x}\end{aligned}$$

When these are used in the governing equations, the continuity equation is automatically satisfied, and the momentum equations become:

$$\nabla^2 \Psi = -\zeta \quad (15)$$

$$\nabla^2 \zeta = R_e \left( \frac{\partial u \zeta}{\partial x} + \frac{\partial v \zeta}{\partial y} \right) \quad (16)$$

## BEM-GIF Equations

We distribute sources of strength  $\omega_1$  (for  $\Psi$ ) and  $\omega_2$  (for  $\zeta$ ) on the boundary  $\Gamma$ . The complete solution can be written in the form:

$$\Psi(\mathbf{x}) = \int_{\Gamma} \omega_1(\mathbf{x}') d\mathbf{x}' + \sum_k \beta_{1k} \Phi_k(\mathbf{x}) \quad (17)$$

$$\zeta(\mathbf{x}) = \int_{\Gamma} \omega_2(\mathbf{x}') d\mathbf{x}' + \sum_k \beta_{2k} \Phi_k(\mathbf{x}) \quad (18)$$

The coefficients  $\beta_{ik}$  ( $i = 1, 2$ ) are determined by enforcing equations (15) and (16) at select collocation points, while  $\omega_i$  ( $i = 1, 2$ ) are determined by enforcing the boundary conditions.

## 3D Primitive Variable Formulation

The governing equations are

$$\frac{\partial u}{\partial x} + \frac{\partial v}{\partial y} + \frac{\partial w}{\partial z} = 0 \quad (19)$$

$$u \frac{\partial u}{\partial x} + v \frac{\partial u}{\partial y} + w \frac{\partial u}{\partial z} = -\frac{\partial p}{\partial x} + \frac{1}{R_e} \left( \frac{\partial^2 u}{\partial x^2} + \frac{\partial^2 u}{\partial y^2} + \frac{\partial^2 u}{\partial z^2} \right) \quad (20)$$

$$u \frac{\partial v}{\partial x} + v \frac{\partial v}{\partial y} + w \frac{\partial v}{\partial z} = -\frac{\partial p}{\partial y} + \frac{1}{R_e} \left( \frac{\partial^2 v}{\partial x^2} + \frac{\partial^2 v}{\partial y^2} + \frac{\partial^2 v}{\partial z^2} \right) \quad (21)$$

$$u \frac{\partial w}{\partial x} + v \frac{\partial w}{\partial y} + w \frac{\partial w}{\partial z} = -\frac{\partial p}{\partial z} + \frac{1}{R_e} \left( \frac{\partial^2 w}{\partial x^2} + \frac{\partial^2 w}{\partial y^2} + \frac{\partial^2 w}{\partial z^2} \right) \quad (22)$$

Taking the divergence of the momentum equation and enforcing mass conservation, the pertinent PDE for the pressure is:

$$\begin{aligned}\nabla^2 p &= -2 \left\{ \left( \frac{\partial u}{\partial x} \right) \left( \frac{\partial v}{\partial y} \right) + \left( \frac{\partial u}{\partial x} \right) \left( \frac{\partial w}{\partial z} \right) + \left( \frac{\partial v}{\partial y} \right) \left( \frac{\partial w}{\partial z} \right) \right\} \\ &\quad + 2 \left\{ \left( \frac{\partial u}{\partial y} \right) \left( \frac{\partial v}{\partial x} \right) + \left( \frac{\partial u}{\partial z} \right) \left( \frac{\partial w}{\partial x} \right) + \left( \frac{\partial v}{\partial z} \right) \left( \frac{\partial w}{\partial y} \right) \right\}\end{aligned} \quad (23)$$

## BEM-GIF Equations

The fundamental solution for convection-free three-dimensional must satisfy

$$\nabla^2 g(\mathbf{x}, \mathbf{x}') = 4\pi \delta(\mathbf{x}, \mathbf{x}')$$

where  $\delta$  is the Dirac delta function applied at point  $\mathbf{x} = (x, y, z)$ , and felt at the point  $\mathbf{x} = (x', y', z')$ . The closed form solution for  $g$  is easily shown to be (Jaswon & Symm [1977])

$$g = \frac{1}{r}$$

where  $r = |\mathbf{x} - \mathbf{x}'|$ .

The full solution can be written in the form

$$\begin{aligned} u(\mathbf{x}) = & \int_{\Gamma} \omega_1(\mathbf{x}') g_{11}(\mathbf{x}, \mathbf{x}') d\Gamma \\ & + \int_{\Gamma} \omega_2(\mathbf{x}') g_{12}(\mathbf{x}, \mathbf{x}') d\Gamma \\ & + \int_{\Gamma} \omega_3(\mathbf{x}') g_{13}(\mathbf{x}, \mathbf{x}') d\Gamma \\ & + \sum_k \beta_{1k} \Phi_{k11}(\mathbf{x}) \\ & + \sum_k \beta_{2k} \Phi_{k12}(\mathbf{x}) \\ & + \sum_k \beta_{3k} \Phi_{k13}(\mathbf{x}) \end{aligned} \quad (24)$$

$$\begin{aligned} v(\mathbf{x}) = & \int_{\Gamma} \omega_1(\mathbf{x}') g_{21}(\mathbf{x}, \mathbf{x}') d\Gamma \\ & + \int_{\Gamma} \omega_2(\mathbf{x}') g_{22}(\mathbf{x}, \mathbf{x}') d\Gamma \\ & + \int_{\Gamma} \omega_3(\mathbf{x}') g_{23}(\mathbf{x}, \mathbf{x}') d\Gamma \\ & + \sum_k \beta_{1k} \Phi_{k21}(\mathbf{x}) \\ & + \sum_k \beta_{2k} \Phi_{k22}(\mathbf{x}) \\ & + \sum_k \beta_{3k} \Phi_{k23}(\mathbf{x}) \end{aligned} \quad (25)$$

$$\begin{aligned} w(\mathbf{x}) = & \int_{\Gamma} \omega_1(\mathbf{x}') g_{31}(\mathbf{x}, \mathbf{x}') d\Gamma \\ & + \int_{\Gamma} \omega_2(\mathbf{x}') g_{32}(\mathbf{x}, \mathbf{x}') d\Gamma \\ & + \int_{\Gamma} \omega_3(\mathbf{x}') g_{33}(\mathbf{x}, \mathbf{x}') d\Gamma \\ & + \sum_k \beta_{1k} \Phi_{k31}(\mathbf{x}) + \beta_{2k} \Phi_{k32}(\mathbf{x}) \\ & + \sum_k \beta_{3k} \Phi_{k33}(\mathbf{x}) \end{aligned} \quad (26)$$

$$\begin{aligned} p(\mathbf{x}) = & \int_{\Gamma} \omega_4(\mathbf{x}') g_{44}(\mathbf{x}, \mathbf{x}') d\Gamma \\ & + \sum_k \beta_{4k} \Phi_{k44} \end{aligned} \quad (27)$$

**Sources/Dipoles** By selecting  $g_{11} = g_{22} = g_{33} = g_{44} = g = 1/r$  and enforcing continuity, the functions  $g_{ij}$  ( $i \neq j$ ) are given by:

$$\begin{aligned} g_{12} &= \frac{(x - x')(y - y')}{r_{yz}r} \\ g_{13} &= \frac{(x - x')(z - z')}{r_{yz}r} \\ g_{21} &= \frac{(x - x')(y - y')}{r_{xz}r} \\ g_{23} &= \frac{(y - y')(z - z')}{r_{xz}r} \\ g_{31} &= \frac{(x - x')(z - z')}{r_{xy}r} \\ g_{32} &= \frac{(y - y')(z - z')}{r_{xy}r} \end{aligned}$$

where

$$r_{xy} = (x - x')^2 + (y - y')^2$$

$$r_{xz} = (x - x')^2 + (z - z')^2$$

and

$$r_{yz} = (y - y')^2 + (z - z')^2$$

**GIF Bases** If  $\Phi_{k11} = \Phi_{k22} = \Phi_{k33} = \Phi_{k44} = \cosh(m_k x) \cosh(n_k y) \cosh(l_k z)$  then for mass to be automatically conserved, the auxiliary functions  $\Phi_{kij}$  ( $i \neq j$ ) are given by:

$$\begin{aligned} \Phi_{k12} &= -\frac{n_k}{2m_k} \sinh(m_k x) \sinh(n_k y) \cosh(l_k z) \\ \Phi_{k13} &= -\frac{l_k}{2m_k} \sinh(m_k x) \cosh(n_k y) \sinh(l_k z) \\ \Phi_{k21} &= -\frac{m_k}{2n_k} \sinh(m_k x) \sinh(n_k y) \cosh(l_k z) \\ \Phi_{k23} &= -\frac{l_k}{2n_k} \cosh(m_k x) \sinh(n_k y) \sinh(l_k z) \\ \Phi_{k31} &= -\frac{m_k}{2l_k} \sinh(m_k x) \cosh(n_k y) \sinh(l_k z) \\ \Phi_{k32} &= -\frac{n_k}{2l_k} \cosh(m_k x) \sinh(n_k y) \sinh(l_k z) \end{aligned}$$

Similar auxiliary functions can be derived for other selections of GIF such as

1. Polynomial  $x^m y^n z^l$ ;
2. Trigonometric  $\cos(mx) \cos(ny) \cos(lz)$ ; and
3. Radial  $1 + r^{2(m+1)}$  functions.

### 3D Velocity-Vorticity Formulation

The vorticity vector  $\hat{\zeta} = (\zeta_x, \zeta_y, \zeta_z)$  is defined by

$$\hat{\zeta} = \nabla \times \mathbf{u}$$

where  $\nabla \times$  is the curl operator. Using the above in conjunction with the continuity equation  $\nabla \cdot \mathbf{u} = 0$  the following Poisson equations can be derived for the velocity components:

$$\nabla^2 u = \partial \zeta_y / \partial z - \partial \zeta_z / \partial y \quad (28)$$

$$\nabla^2 v = \partial \zeta_z / \partial x - \partial \zeta_x / \partial z \quad (29)$$

$$\nabla^2 w = \partial \zeta_x / \partial y - \partial \zeta_y / \partial x \quad (30)$$

where  $\mathbf{x} = (x, y, z)$  is the spatial coordinate.

The three-component vorticity transport equation is (Fletcher [1991])

$$\nabla \cdot (\mathbf{u} \hat{\zeta}) - (\hat{\zeta} \cdot \nabla) \mathbf{u} - \frac{1}{Re} \nabla^2 \hat{\zeta} = 0 \quad (31)$$

For three-dimensional flows, there are six equations for  $u, v, w, \zeta_x, \zeta_y, \zeta_z$ . These equations are expressible in the general elliptical form:

$$\nabla^2 \Theta = \mathbf{f} \quad (32)$$

where  $\Theta = (\theta_1, \theta_2, \dots, \theta_6)$ ,  $\theta_1 = u$ ,  $\theta_2 = v$ ,  $\theta_3 = w$ ,  $\theta_4 = \zeta_x$ ,  $\theta_5 = \zeta_y$ ,  $\theta_6 = \zeta_z$ , and  $\mathbf{f} = (f_1, f_2, \dots, f_6)$ , with:

$$\begin{pmatrix} f_1 \\ f_2 \\ f_3 \\ f_4 \\ f_5 \\ f_6 \end{pmatrix} = \begin{pmatrix} \frac{\partial \zeta_y}{\partial z} - \frac{\partial \zeta_z}{\partial y} \\ \frac{\partial \zeta_z}{\partial x} - \frac{\partial \zeta_x}{\partial z} \\ \frac{\partial \zeta_x}{\partial y} - \frac{\partial \zeta_y}{\partial x} \\ Re(\xi_{11} - \xi_{12}) \\ Re(\xi_{21} - \xi_{22}) \\ Re(\xi_{31} - \xi_{32}) \end{pmatrix} \quad (33)$$

$$\xi_{11} = \frac{\partial u \zeta_x}{\partial x} + \frac{\partial v \zeta_x}{\partial y} + \frac{\partial w \zeta_x}{\partial z}$$

$$\xi_{12} = \zeta_x \frac{\partial u}{\partial x} + \zeta_y \frac{\partial u}{\partial y} + \zeta_z \frac{\partial u}{\partial z}$$

$$\xi_{21} = \frac{\partial u \zeta_y}{\partial x} + \frac{\partial v \zeta_y}{\partial y} + \frac{\partial w \zeta_y}{\partial z}$$

$$\xi_{22} = \zeta_x \frac{\partial v}{\partial x} + \zeta_y \frac{\partial v}{\partial y} + \zeta_z \frac{\partial v}{\partial z}$$

$$\xi_{31} = \frac{\partial u \zeta_z}{\partial x} + \frac{\partial v \zeta_z}{\partial y} + \frac{\partial w \zeta_z}{\partial z}$$

$$\xi_{32} = \zeta_x \frac{\partial w}{\partial x} + \zeta_y \frac{\partial w}{\partial y} + \zeta_z \frac{\partial w}{\partial z}$$

### BEM/GIF Equations

We write the solution in the form:

$$\theta_i(\mathbf{x}) = \int_{\Gamma} \omega_i(\mathbf{x}') g(\mathbf{x}, \mathbf{x}') d\mathbf{x}' + \sum_k \beta_{ik} \Phi_k(\mathbf{x}) \quad (34)$$

$i = 1, 2, \dots, 6$

where  $g$  is the free-space Green's function for the Laplace's equation (i.e., convection-free flow).

The coefficients  $\beta_{ik}$  are determined by enforcing the governing equations at select collocation points, while the strengths  $\omega_i$  of the fictitious boundary sources are determined by enforcing the boundary conditions.

### Numerical Implementation

Regardless of which formulation is used, the above BEM-GIF schemes share a common pattern: each solution consists of a sum of a boundary integral and a finite series. The numerical implementation can also be generalized for all the formulations.

Consider the flow variable  $\theta$ . We subdivide the boundary into  $n_b$  elements. Let  $N_j(\mathbf{x})$  ( $j = 1, 2, \dots, n_b$ ) represent the basis functions describing the distribution of  $\omega$  on  $\Gamma$ .

#### Source/Vortex Strength Determination

By selecting each of the  $n_b$  boundary points as successive origins of integration, the pertinent integral equations can be assembled into the system:

$$\sum_{j=1}^{n_b} \sum_{k=1}^{n_\omega} a_{ikj} \omega_{kj} = b_i \quad i = 1, 2, \dots, n_b \quad (35)$$

where  $n_\omega$  is the number of source/vortex combinations used to model the flow variable, and

$$a_{ikj} = \begin{cases} \int_{\Gamma} N_j(\mathbf{x}') g_{ikj}(\mathbf{x}', \mathbf{x}_i) d\mathbf{x}' & \mathbf{x}_i \in \Gamma_\theta \\ \int_{\Gamma} N_j(\mathbf{x}') \frac{\partial g_{ikj}}{\partial n}(\mathbf{x}', \mathbf{x}_i) d\mathbf{x}' & \mathbf{x}_i \in \Gamma_q \end{cases} \quad (36)$$

$$b_i = \begin{cases} \theta(\mathbf{x}_i) - \sum_{k=1}^{n_d} \sum_{j=1}^{n_\omega} \beta_{jk} \Phi_{ikj} & \mathbf{x}_i \in \Gamma_\theta \\ \frac{\partial \theta}{\partial n}(\mathbf{x}_i) - \sum_{k=1}^{n_d} \sum_{j=1}^{n_\omega} \beta_{jk} \frac{\partial \Phi_{ikj}}{\partial n} & \mathbf{x}_i \in \Gamma_q \end{cases} \quad (37)$$

where  $\Gamma_\theta$  is the boundary segment on which the variable  $\theta$  is prescribed while  $\Gamma_q$  is the portion on which  $\partial\theta/\partial n = \nabla\theta \cdot \mathbf{n}$  is prescribed.

Therefore, we have  $n_b n_\omega$  equations to determine  $\omega_{jk}$  ( $j = 1, 2, \dots, n_b$ ;  $k = 1, 2, \dots, n_\omega$ ). Symbolically equation (35) can be written in the alternative form:

$$[A]\{W\} = \{B\} \quad (38)$$

which can be inverted to give:

$$\{W\} = [A]^{-1} \{B\} \quad (39)$$

### GIF Coefficients Determination

The algebraic equations for determining the GIF coefficients  $\beta$  are nonlinear, on account of the convective terms. Therefore, the solution process has to be iterative. We start by assuming a convection-free flow, so that all the  $\beta$  values are set to zero initially. We then compute the error  $\varepsilon$  in the transport equation for  $\theta$  at each of the  $n_d$  collocation points. The error  $\Delta\theta$  is assumed to be related to  $\varepsilon$  through

$$\Delta\theta = \lambda\varepsilon$$

where  $\lambda$  is a relaxation parameter. The error  $\Delta\theta$  is a function of the errors in the GIF coefficients. That is:

$$\Delta\theta = \sum_{k=1}^{n_d} \sum_{j=1}^{n_\omega} \Delta\beta_{jk} \Phi_{jk} \quad (40)$$

Hence, by computing  $\Delta\theta$  for all  $n_d$  points and all flow variables we have a system of equations:

$$[\Phi]\{\Delta\beta\} = \{\lambda\varepsilon\} \quad (41)$$

which when inverted gives:

$$\{\Delta\beta\} = [\Phi]^{-1} \{\lambda\varepsilon\} \quad (42)$$

The iterative steps are:

1. Start with a trial  $\beta_k$  ( $k = 1, 2, \dots, n_d$ ) for all flow variables. We have found a zero initial value to be the most convenient.
2. Obtain  $W$  using equation (39).

3. Use discretized forms of the appropriate integral equations to compute  $\theta$ ,  $\nabla\theta$  at all  $n_d$  points.
4. Compute the error  $\varepsilon$  in the transport equation at each of the collocation points.
5. Use equation (42) to compute new values of  $\beta$ .
6. Go back to Step 2 if convergence condition is still unsatisfied.

Note that the matrix inversions in equations (39) and (42) need only be performed once, for fixed boundary problems. The vectors  $W$  and  $\beta$  are the quantities whose values change during the iterative process. Once convergence is reached, the discretized integral equations can be used routinely to obtain  $\theta = (u, v, w, p, \Psi, \zeta_x, \zeta_y, \zeta_z)$  or the gradient at any point ( $\mathbf{x}$ ) of interest.

### BEM Codes & Preliminary Tests

Four boundary element codes were developed. These include:

1. **PRIM-2D** This is a two-dimensional general purpose boundary element solver based on the use of primitive variables. The code can be applied to any geometry. Benchmark tests used global interpolation functions drawn from families of trigonometric, hyperbolic, radial, polynomial, wavelet, and Chebychev functions.
2. **VORT-2D** This a two-dimensional code based on a streamfunction-vorticity formulation. The GIF bases enumerated in (1) were tested.
3. **PRIM-3D** This a full three-dimensional boundary element code using primitive variables. Four momentum equations are solved for the three velocity components ( $u, v, w$ ) and the pressure ( $p$ ).
4. **VORT-3D** A full three-dimensional code based on the vorticity-velocity formulation. Six transport equations are solved for the

three vorticity components ( $\zeta_x, \zeta_y, \zeta_z$ ) and the three velocity components ( $u, v, w$ ).

Typical performance test results using PRIM-2D for the lid-driven cavity problem (Fig. 1) are shown in Figs. 2-3. The number of boundary elements  $n_b = 64$  (i.e., 8 per side); and the number of collocation points  $n_d = 64$ . The test results shown were obtained using the following relaxation parameters:

$$\begin{aligned}\lambda_u &= 0.2 \\ \lambda_p &= 0.02 \\ \lambda_w &= 1.0\end{aligned}$$

Preliminary test runs on three-dimensional developing flows in straight and curved square ducts (Fig. 4) were also carried out. We set  $a = b = 1$ ;  $R = 10$ , and  $\alpha = \pi/2$ . We assumed a plug flow ( $u = 1$ ;  $v = w = 0$ ) at the inlet. A total of 72 rectangular boundary elements and 343 internal nodes were used. Other salient parameters include:

$$\begin{aligned}\lambda_u = \lambda_v = \lambda_w = \lambda_\omega &= 0.001 \\ \lambda_p &= 1.0 \\ R_e &= 1000\end{aligned}$$

The velocity convergence characteristics of VORT-3D for the curved square duct is shown in Fig. 5.

This is an ongoing research effort. We plan to report the comprehensive performance characteristics of all four BEM modules in an upcoming publication.

## Conclusions

The paper presents the general foundation for obtaining boundary integral solutions to incompressible viscous flows. The GIF-based boundary integral equations ensure the automatic conservation of mass. Critical factors which affect the convergence rates and the quality of the solutions include:

1. The choice of the relaxation parameter  $\lambda$  as a function of the Reynold's number  $R_e$ , the number of boundary elements  $n_b$ , the number of collocation points  $n_d$ , the domain size

$L$ , and other parameters that may influence the flow problem. The convergence rate is highly sensitive to the choice of  $\lambda$ .

2. The optimal location of the collocation points  $x_k$  ( $k = 1, 2, \dots, n_d$ ) so that the ensuing solution process will capture the underlying physics of the problem. It is clear that  $n_d$  can be much smaller than the number of computational nodes required in the domain methods (e.g., finite elements and finite differences). However, since we are at liberty to select these points, their optimal location is crucial, in order to exploit the inherent advantages of the BEM-GIF formulation.

## Acknowledgments

This research work is being supported by NASA Lewis Research Center, under the Contract NAS3-27019.

## References

1. Brebbia, C.A., *Two Different Approaches for Transforming Domain Integrals to the Boundary*, Mathl Comput. Modelling, Vol. 15, No. 3-5, pp. 43-58, 1991.
2. Brebbia, C.A., J.C.F. Telles, and L.C. Wrobel, **Boundary Element techniques - Theory and applications in Engineering**, Springer-Verlag, 1984.
3. Cheng, A. H-D., S. Grilli, and O. Lafe, *Dual Reciprocity Boundary Element Based on Global Interpolation Functions*, Eng. Analysis with Boundary Elements, to appear, 1994.
4. Cheng, A. H-D., and D. Ouazar, *Groundwater*, Chapter 9 in **Boundary Element Techniques in Geomechanics**, eds. G.D. Manolis and T.G. Davies, CMP/Elsevier, 1993.
5. Fletcher, C.A.J., **Computational Techniques for Fluid Dynamics**, Vol. II (pg. 391), Springer-Verlag, 1991.



6. Greenberg. M.D..  
**Applications of Green's Functions in Science and Engineering**, Prentice-Hall, Englewood Cliffs, New Jersey, 1971.
7. Jaswon, M.A., and G.T. Symm, *Integral Equation Methods in Potential Theory and Elastostatics*, Academic, San Diego, Calif., 1977.
8. Lafe, O., *A Dual Reciprocal Boundary element Formulation for Viscous Flows*, in Proc. NASA Fifth Annual Thermal and Fluids Analysis Workshop (NASA Conference Publication 10122), Brook Park, Aug. 16-20, 1993.
9. Lafe, O., and A. H-D. Cheng, *A Global Interpolation Function Based Boundary Element Method for Deterministic, Non-homogeneous, and Stochastic Flows in Porous Media*, Computers and Structures, To Appear, 1994.
10. Nardini, D., and C.A. Brebbia, *A New Approach to Free Vibration Analysis using Boundary Elements*, in **Boundary Element Methods in Engineering**, Proc. 4th Int. Sem., Southampton, ed. C.A. Brebbia. Springer-Verlag, 312-326, 1982.
11. Partridge. P.W., C.A. Brebbia, and L.C. Wrobel. *The Dual Reciprocity Boundary Element Method*, CMP/Elsevier, 1992.

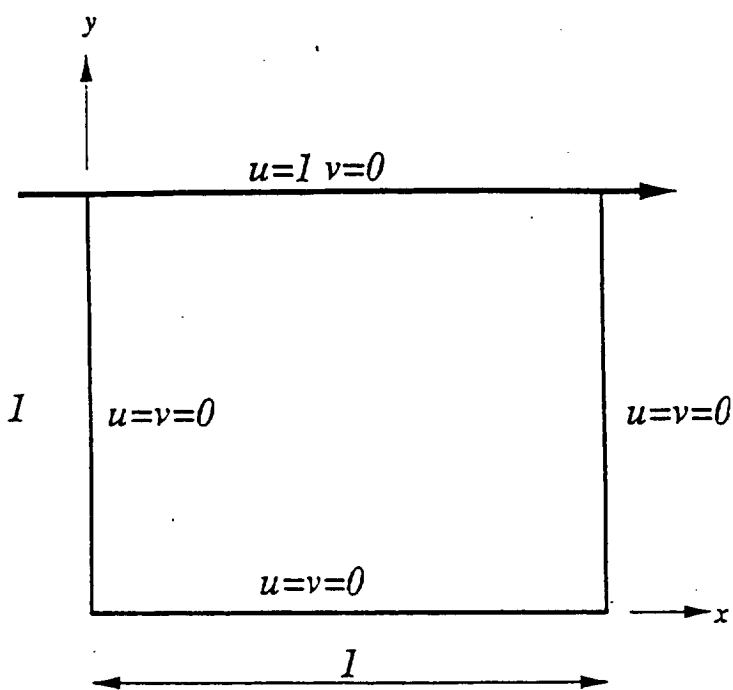


Figure 1: Lid-driven Cavity Problem

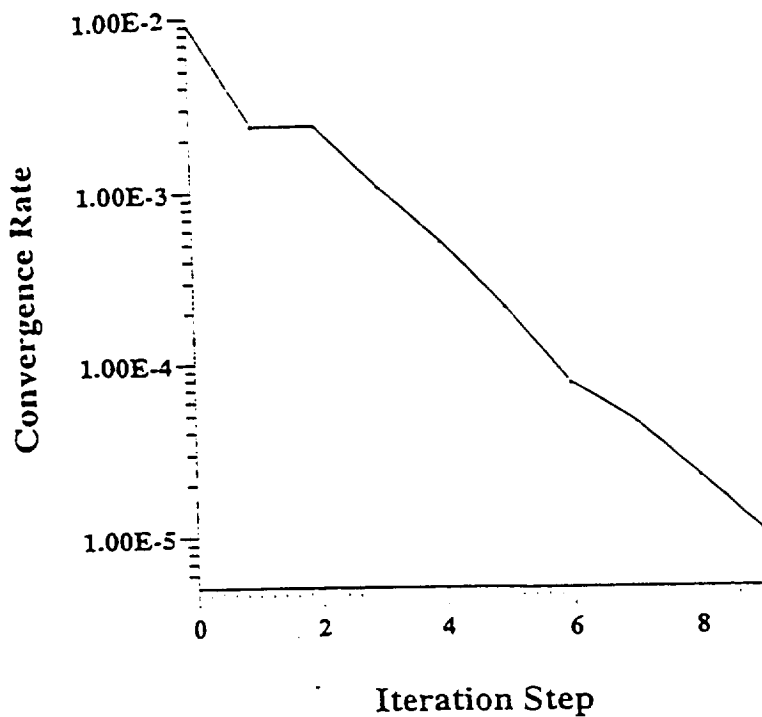


Figure 2: Velocity Convergence Rate for Cavity Problem

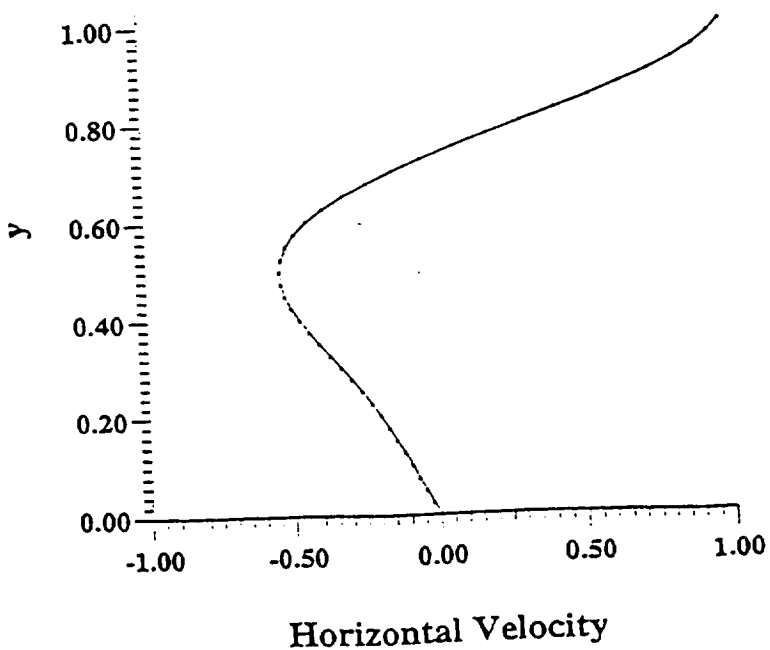


Figure 3: Centerline Velocity Profile for Cavity Problem

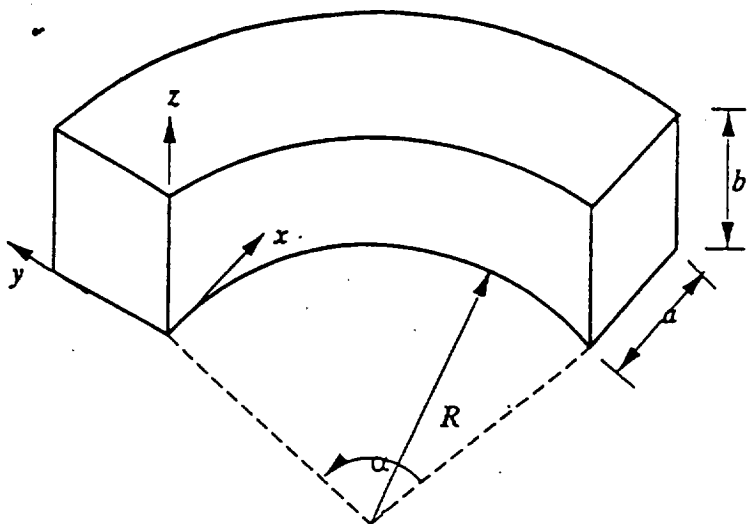


Figure 4: Curved Square Duct Problem

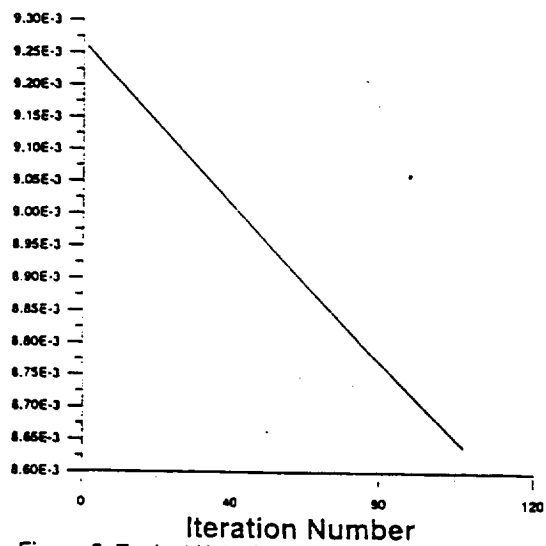


Figure 5: Typical Velocity Convergence Rate for Curved Square Duct